BNL--40717

DE88 006365

BNL 40717

CONF-870739--17

DISCLAIMER

This report was prepared as an account of work sponsored by an agency of the United States Government. Neither the United States Government nor any agency thereof, nor any of their employees, makes any warranty, express or implied, or assumes any legal liability or responsibility for the accuracy, completeness, or usefulness of any information, apparatus, product, or process disclosed, or represents that its use would not infringe privately owned rights. Reference herein to any specific commercial product, process, or service by trade name, trademark, manufacturer, or otherwise does not necessarily constitute or imply its endorsement, recommendation, or favoring by the United States Government or any agency thereof. The views and opinions of authors expressed herein do not necessarily state or reflect those of the United States Government or any agency thereof.

UCSB-HEP-87-15

REPORT OF THE INTERMEDIATE-$p_\perp$ DETECTOR GROUP: A BEAUTY SPECTROMETER FOR THE SSC

K. J. Foley
Brookhaven National Laboratory, Upton, Long Island NY 11973 *
C. D. Buchanan
University of California, Los Angeles CA 90024
R. J. Morrison, S. W. McHugh, and M. S. Witherell
University of California, Santa Barbara CA 93106
M. Atac, B. Cox, M. V. Purohit, R. Stefanski, and D. E. Wagoner
Fermilab, Batavia IL 60510
K. Schubert
Heidelberg University, Heidelberg, FRG
L. W. Jones
University of Michigan, Ann Arbor MI 48109
I. Leedom
Northeastern University, Boston MA 02115
D. A. Buchholz
Northwestern University, Evanston IL 60201
N. W. Reay
Ohio State University, Columbus OH 43210
N. Lockyer
University of Pennsylvania, Philadelphia PA 19104
S. N. White
Rockefeller University, New York NY 10021
V. G. Lüth and S. L. Shapiro
Stanford Linear Accelerator Center, Stanford CA 94305
D. E. Groom
Superconducting Super Collider Central Design Group, Berkeley CA 94720
A. Jawahery
Syracuse University, Syracuse NY 13244
P. Karchin, M. P. Schmidt, and J. Slaughter
Yale University, New Haven CT 06511

* Research carried out under the auspices of the U.S. Department of Energy under Contract No. DE-AC02-76CH00016.

MASTER

DISTRIBUTION

REPORT OF THE INTERMEDIATE-$p_\perp$ DETECTOR GROUP: A BEAUTY SPECTROMETER FOR THE SSC

K. J. Foley
Brookhaven National Laboratory, Upton, Long Island NY 11973
C. D. Buchanan
University of California, Los Angeles CA 90024
R. J. Morrison, S. W. McHugh, and M. S. Witherell
University of California, Santa Barbara CA 93106
M. Atac, B. Cox, M. V. Purohit, R. Stefanski, and D. E. Wagoner
Fermilab, Batavia IL 60510
K. Schubert
Heidelberg University, Heidelberg, FRG
L. W. Jones
University of Michigan, Ann Arbor MI 48109
I. Leedom
Northeastern University, Boston MA 02115
D. A. Buchholz
Northwestern University, Evanston IL 60201
N. W. Reay
Ohio State University, Columbus OH 43210
N. Lockyer
University of Pennsylvania, Philadelphia PA 19104
S. N. White
Rockefeller University, New York NY 10021
V. G. Lüth and S. L. Shapiro
Stanford Linear Accelerator Center, Stanford CA 94305
D. E. Groom
Superconducting Super Collider Central Design Group, Berkeley CA 94720
A. Jawahery
Syracuse University, Syracuse NY 13244
P. Karchin, M. P. Schmidt, and J. Slaughter
Yale University, New Haven CT 06511

A "Beauty Spectrometer" has been designed for studies of B physics at the SSC. The ultimate goal is a definitive measurement of CP violation in the B system. The spectrometer consists of two stages and occupies one side of an intermediate-luminosity interaction region. An upstream, or intermediate, stage extends from the interaction point to 14 m and covers the angular region from 57 mrad (3.3°) to 350 mrad (20°). The forward stage extends to 77 m and to angles down to 5.7 mrad. The design includes silicon microstrip detectors, conventional tracking, momentum analysis, and hadron and lepton identification. While no fundamental problems have been found, the detector must deal with unprecedented particle fluxes, trigger rates, and data rates.

1. Introduction

The great majority of the intermediate-$p_\perp$ group worked as one subgroup on one problem—a spectrometer for bottom quark physics. The members of this effort set out to make a trial design of a forward beauty spectrometer capable of decisively observing CP violation at the level expected in the standard model. The theoretical groundwork was provided by the B physics group, whose report is contained in this volume [1]. Although there has been a great deal of interest in various techniques for obtaining large samples of B-meson decays, it is doubtful that any of them will be sufficient for studying CP violation before the SSC is operating. Even though there are still many experimental questions that require further study, it was possible to produce a rough design that is not obviously inadequate. It should serve as a good starting point for more detailed studies in the future, which can concentrate on the critical problems pointed out in this study.

Since the forward beauty spectrometer subgroup included most of the members of the intermediate $p_\perp$ group, its description makes up the bulk of this report. Two smaller smaller groups worked on the problem of electron and muon triggers for the B-physics experiment. The description of the electron trigger [2] is included in this volume as a separate contribution. It is treated separately in part to emphasize the fact that the lepton triggers are crucial for the success of the experiment and by themselves present difficult problems that need more attention.

Other members of the intermediate-$p_\perp$ group worked on three spectrometers, which are described in a separate paper [3]. These designs address experimental goals not well matched to the general purpose detectors, and which are discussed in detail in the report. In addition, L. W. Jones considered instrumentation of the forward cone inside that covered by the beauty spectrometer; his design is also presented separately [4].

2. B Physics at the SSC

There is a great deal of interest in the bottom quark system as a source of information on CP violation. In contrast to the charm case, bottom can only decay outside the top-bottom family, greatly enhancing the sensitivity to CP violation. The recent observation of mixing for B_d^0 has generated still more interest in the possibility for observing CP violating effects, since the size of these effects is now expected to be substantially larger.

In the bottom system CP violating effects are expected to appear in many decay modes, but as a general pattern the largest asymmetries occur for modes with extremely small branching ratios. As a result, an experiment must be

exposed to a very large number of B's in order to guarantee making a clear statement about CP violation.

The cleanest predictions of CP violating effects occur for decays into CP eigenstates. In these cases, CP violation is observed by comparing the decay time distributions of the CP eigenstates, using the other B to tag whether a particle or antiparticle is decaying. For example, the final state for B (or $\overline{\mathrm{B}}$) $\rightarrow \psi \mathrm{K}_s \mathrm{X}$ is tagged as CP = +1 by the fast 2π decay of the K_s, while the leptonic decay of the other B identifies the parent as a B or $\overline{\mathrm{B}}$. The asymmetry $(\mathrm{N(B)} - \mathrm{N}(\overline{\mathrm{B}}))/(\mathrm{N(B)} + \mathrm{N}(\overline{\mathrm{B}}))$ is expected to be between 0.05 and 0.3 if the violation arises through the phase angle δ in the Kobayashi-Maskawa matrix, large enough to be measured with relative freedom from systematic errors if enough events are available. With the expected branching ratios, tagging efficiency, and other penalties, the asymmetry can be measured at the 3σ level with less than 10^8 B's.

The total cross section for $\mathrm{B}\overline{\mathrm{B}}$ production at the SSC is expected to lie in the range 200 μb to 700 μb.* The spectrometer we envisage makes use of an intermediate-length interaction region, where the luminosity is $10^{32}\,\mathrm{cm}^{-2}\mathrm{s}^{-1}$. The $\mathrm{B}\overline{\mathrm{B}}$ production rate is then (2 to 7) $\times\, 10^4\,\mathrm{s}^{-1}$, for a total of (2 to 7) $\times\, 10^{11}$ in a nominal year of running. The rapidity distribution is expected to be fairly flat out to 5 or 6.†

Given the prodigious rates and rich physics, $\mathrm{B}\overline{\mathrm{B}}$ studies promise to be an important part of the SSC program. They are also very difficult. The $\mathrm{B}\overline{\mathrm{B}}$ rate is already formidable, but the total p-p interaction rate is about 500 times greater, with roughly the same rapidity distribution. The spectrometer must operate at unprecedentedly high rates, there is an extreme demand on triggering and readout electronics, and there must be an enormous capability for data transfer and data reduction. To investigate the possibilities and problems of these rates,

---

* We take 200 μb as the "standard" $\mathrm{B}\overline{\mathrm{B}}$ production cross section for purposes of this report. This cross section is to be compared with the 1.1 μb cross section measured at the $\mathrm{S}\overline{\mathrm{p}}\mathrm{pS}$. The SSC luminosity contributes several additional orders of magnitude to the rate.

† The rapidity y is defined as

$$y = \tfrac{1}{2} \ln \frac{E + p_{\parallel}}{E - p_{\parallel}}$$
$$= \tfrac{1}{2} \ln \frac{\cos^2(\theta/2) + m^2/4p^2 + \cdots}{\sin^2(\theta/2) + m^2/4p^2 + \cdots} .$$

If terms of order $(m/p)^2$ and higher can be neglected, the function depends only upon angle and is called the *pseudorapidity* η. The approximation $y \approx \eta$ breaks down for low energy particles and for angles smaller than $m/p \approx 1/\gamma$. Because of its greater relevance to experimental design, pseudorapidity is used for the remainder of this report.

we have made a first pass at the design of a specialized detector for B physics at the SSC. Our goal was to make a detector which would be as sensitive as possible to CP violation in as many modes as possible, and, in addition, to be sensitive in general to rare B decays. It followed immediately that high precision vertex finding and both hadron and lepton particle identification are required.

Triggering is an extremely difficult problem. In addition to the J/ψ trigger which has been previously discussed[5], we attempted to make a spectrometer which includes electron and muon triggers. The trigger lepton provides a particle-antiparticle tag if the associated D is reconstructed, allowing for a wide variety of detectable decay modes for the other B.

3. Design Considerations

i. Acceptance

If the distribution in rapidity (actually pseudorapidity) $dN/d\eta$ is taken as a constant (C), then $|dN/d\theta| = C/\sin\theta$ and $dN/d\Omega = C/(2\pi\sin^2\theta)$. Therefore (a) the distribution of B's (or secondary particles of any kind) is peaked strongly in the forward direction, falling only at angles smaller than 0.7 mrad,* (b) the counting rate in a small counter at a transverse distance R_T from the beam is independent of distance from the interaction point, down to $\theta \approx 5$ mrad ($\eta \approx 6$), and (c) at a fixed distance from the interaction point the counting rate scales as R_T^{-2}.

These considerations led us to a spectrometer occupying the forward region. The length of the detector is well matched to the available free space in the intermediate-luminosity interaction regions planed for the SSC, and the luminosity in these regions is well matched to rate requirements for CP violation studies and other B studies. The forward region is also well matched to the geometry of silicon microstrip detectors, whose resolution is of fundamental importance for heavy flavor identification.

Since both the B and the $\overline{\mathrm{B}}$ must be accepted, there is a high premium on providing a large acceptance. The expected production characteristics of quarks have been described by B. Cox and D. E. Wagoner in 1986[5], and by Foley *et al.* elsewhere in this volume[1]. A broad distribution of B mesons extends to about ± 6 units of rapidity. The b and $\bar{b}$ quarks tend to be produced in the same direction, so the directions of the B and $\overline{\mathrm{B}}$ mesons are highly correlated within about ± 1.5 units of rapidity. The resulting angular distribution of B quarks is strongly peaked in the forward-backward direction with respect to the beams,

* Since $dN/d\eta$ decreases for $\eta \gtrsim 6$.

with both B quarks on the same side.*

To investigate the acceptance of a generic detector, a study was performed simulating the decays of B's into two and three charged particles. The B and $\overline{\mathrm{B}}$ mesons were generated with a $p_\perp$ greater than two GeV/c and in the rapidity interval $-6 < \eta < 6$. The results of this study are shown in Fig. 1. Here increasing the acceptance interval of the "TASTER", ($1° < \theta < 20°$, or $1.74 < \eta < 4.74$)[6], was studied. All of the decay products from both B's fall in the $1°-20°$ acceptance for 8.8% of the events. Keeping the 20° ($\eta = 1.74$) intermediate acceptance and lowering the forward angle to 5 milliradians ($\eta = 6$) increases this fraction to 14%. Keeping the forward acceptance limited to 1° and increasing the outer acceptance to 40° increases the fraction to 15%.

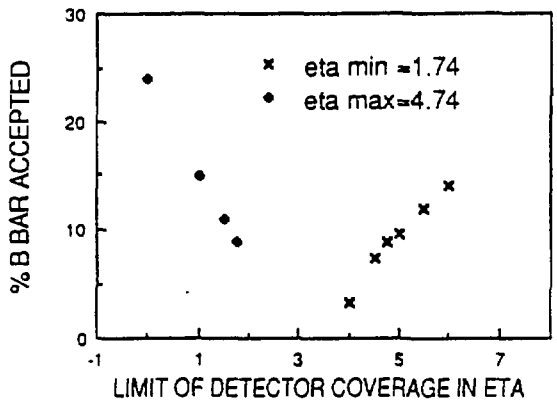

Figure 1. $\mathrm{B\overline{B}}$ acceptance of the 1986 "TASTER" for both B's into two and three body charged modes as the inner and outer acceptance angles are changed. The dots indicate the fraction of events accepted when the outer acceptance angle is varied and the small angle acceptance is fixed at 1°. The crosses correspond to keeping the outer acceptance fixed at 20° and varying the small angle acceptance. The outer acceptance angle of the spectrometer described in this report is the same as that of the "TASTER," but the inner angle (5.7 mrad) corresponds to $\eta \approx 6$.

Clearly the acceptance should be increased both forward and outward as much as possible. In fact, however, it is only the part of the acceptance which has good vertex finding, charge particle reconstructibility, and particle identification. We have accordingly adopted a minimum angle of 5.7 mrad while leaving the outer angle at 20° (350 mrad).

* Because of this, there is little to be gained in covering both directions. The replication of cost and effort would only double the rate.

ii. General considerations

We have mentioned that for a number of reasons an intermediate luminosity of $10^{32}\,\mathrm{cm}^{-2}\mathrm{s}^{-1}$ is appropriate for B physics at the SSC. If we assume current technology (silicon microstrip vertex detectors) for the vertex finding, then the multiple Coulomb scattering limit on the vertex resolution is $\Delta x = 0.014(R_T/p_\perp)\sqrt{X_0}$. In this expression R_T is the transverse distance from the beams, $p_\perp$ is the transverse momentum of the particle in GeV/c, and X_0 is the thickness of the detector in radiation lengths. This limit requires that the vertex detectors be placed within about 1 cm of the beams. With a luminosity of $10^{32}\,\mathrm{cm}^{-2}\mathrm{s}^{-1}$, current detectors could just survive the dose from a year of running, estimated as 3 megarads at 1 cm from the beam and scaling as the inverse square of this distance.

Another reason is that the approximately ± 100 meters of clear space associated with intermediate luminosity regions allows the small angle regions of detectors to be placed at relatively large distances from the beam, where rates and occupancies are tolerable. Assuming that there are 6 ($\approx 2\pi$) charged particles per unit of rapidity, the probability of a hit per interaction in a counter element of area dA at a distance R_T from the beam is dA/R_T^2, and the probability of a hit in a wire chamber cell of transverse width w is $\pi w/R_T$. The 0.0057 rad chosen for the forward acceptance limit corresponds to a hit probability of $5 \times 10^{-4}\,\mathrm{cm}^{-2}$ for a counter located 70 meters from the interaction region. Similarly, a 2 mm multiwire proportional chamber cell cell at this location has a hit probability of 1.5%.

A final luminosity consideration is that of the trigger. Even at $10^{32}\,\mathrm{cm}^{-2}\mathrm{s}^{-1}$ there are 10^7 interactions per second ($\sigma \approx 100$ mb) and $\sim 2 \times 10^4$ $B\overline{B}$ pairs produced each second ($\sigma \approx 200\ \mu$b), of which 3000 s^{-1} are "in aperture." It is already a severe challenge to design a trigger which is both open for $B\overline{B}$ events and which efficiently rejects the 4000 times larger rate of uninteresting events.

Given that the luminosity is limited to $10^{32}\,\mathrm{cm}^{-2}\mathrm{s}^{-1}$, then what determines the small angle acceptance limit? Here a number of factors come in at $\lesssim 10$ mrad. At 0.0057 radians a 0.3 mm thick cylindrical beryllium beam pipe presents about 10% of a radiation length of material. There are probably better shapes than a simple cylinder for the beam pipe, but in any case the beam pipe becomes a serious problem at very small angles. While occupancies and momentum resolution can be improved with still more space and extra magnets, it appears that the ultra-small angular region is not worth the effort. We chose 0.0057 radians as a practical small-angle limit.

A number of experimental problems develop as the large-angle acceptance limit increases. The vertex detector geometry becomes increasingly complicated due to the ± 7 cm length of the collision region. Tracks from different parts

of this region necessarily have large angles with respect to the normal to the silicon detector plane. Since the silicon is much thicker than the strip spacing ($\sim$50 μm), these large-angle tracks produce partial signals from a number of neighboring strips. These small signals may not be distinguished reliably from noise. If they could be, there would still be a worsened position resolution and a larger probability of overlapping hits.

For this design we decided upon particle tracking and vertex finding before the first magnet, using straight tracks (a condition not completely satisfied for very small angle tracks). It is geometrically very difficult to find an arrangement of magnets and tracking devices which finds reliable pre-magnet track segments and also extends to angles larger than about 20 degrees (350 mrad). Finally, particle and especially electron identification becomes more problematic for these rather low $p_\perp$ tracks at the larger angles. While there is clearly a significant gain to be achieved in extending the angular coverage to larger angles, we decided upon a limit of 350 mrad for purposes of this study.

iii. Minimum size of the beam pipe

The minimum allowable size for the beam pipe can be set by a simple criterion: the limiting aperture of the machine should be somewhere else during all phases of the collider operation. It is sufficient to consider the limiting cases of injection and collision. Both the beam size and the finite crossing angle determine the result.

The r.m.s. width of the beam in the x (or y) direction is given by

$$\sigma_{x(y)} = \sqrt{\epsilon_N \beta_{x(y)}/\gamma} \ ,$$

where ϵ_N is the normalized emittance (nominally 1.0×10^{-6} m-rad), β is the transverse or betatron amplitude function, and γ is the usual Lorentz factor. The optics in the arcs is always the same, with $\beta = 388$ m, and the beam pipe radius is 1.65 cm. During injection β in the interaction region (IR) varies from 60 m at the interaction point (IP) to 320 m at the quadrupole entrance 120 m away. Scaling the arc beam pipe radius by $\sqrt{\beta}$, we find a limiting *inside* radius of 0.7 cm at the IP and 1.4 cm at the quadrupole entrance. Halfway between (60 m) β is about 12 m, so the limiting *inside* radius is 1.0 cm.

After acceleration, the beams are smaller by a factor of $\sqrt{20}$ because of the change in the Lorentz factor. β reaches a very large maximum (2600 m) in the IR quadrupoles. A limiting aperture here would be intolerable for background reasons, so scrapers are moved into place elsewhere in the machine. As a result, the injection optics discussed above still determine the limiting beam pipe

dimensions, even though β at the quadrupole entrance is actually larger in the collision optics configuration.

The crossing angle (α) of the beams is 70 μrad in both the high- and intermediate-luminosity IRs, and for a variety of reasons it cannot be decreased much further. Thus $\alpha/2 \times 120$ m $= 0.42$ cm must be added to the vertical clearance at the quadrupole entrance. The addition scales linearly with distance from the IP.

These results are summarized in Table 1.

Table 1

Minimum inside dimensions of the beam pipe in an intermediate-luminosity interaction region. Alignment errors are assumed to be zero.

Distance from IP	r_x	r_y
0 m	0.7 cm	0.7 cm
60 m	1.0 cm	1.2 cm
120 m	1.4 cm	1.8 cm

iv. Forward and intermediate stages

Given that the occupancy of a detector element depends only upon R_T and is independent of the z position, and given the enormous range of particle momenta, the detector naturally needs to be composed of two, and perhaps even three stages, each covering an optimal rapidity range. Two stages were chosen to avoid the extra edge. Given two stages, the hole into the forward stage, should be made as large as possible. For $dN/d\eta \approx 6$ the occupancy of the edge is $2\pi\Delta R_T/R_T$, where ΔR_T is the edge thickness as defined by electromagnetic and hadronic transverse shower thicknesses.

A large hole is also advantageous for detecting K_s's. This is particularly important since ψK_s is one of the prime CP violation modes. We assume that to be observed a K_s must decay before or within a magnet. This leads to a reduced K_s efficiency for the rather fast K_s's which are just outside of the maximum forward spectrometer acceptance angle. Particles analyzed by the forward stage have much better tracking and particle identification and have a much better momentum resolution.

The cost of the downstream detector limits the size of the hole. The 0.057 radian choice for the hole very roughly bisects the rapidity ranged covered by the detector, with an average of 11 charged particles going into the intermediate detectors and 14 through the hole into the forward stage.

v. Trigger

As discussed in the 1986 Summer Study [5], the B$\rightarrow \psi X \rightarrow \ell^+\ell^- X$ is a clean trigger which is fairly easy to implement. However, this branching ratio with ψ going into either $\mu^+\mu^-$ or e^+e^- is only 7×10^{-4}. The semileptonic B branching ratio into a muon or into an electron is about 10%, more than 100 times larger than for the B $\rightarrow \psi \rightarrow \ell^+\ell^-$ case. In addition, the lepton plus an associated and reconstructed D clearly tags the particle-antiparticle character of the B meson (CP violation is then determined by a study of the time evolution of the "other" B meson). It is thus strongly desirable to trigger on a single electron or muon.

To be effective, such a trigger must include reconstruction of the lepton track to the vertex and must require impact parameters of $\gtrsim 200$ μm with respect either to the beam interaction volume or with respect to another found vertex. There will be a large direct charm background for such a trigger, which can be reduced by imposing a $p_\perp \gtrsim 1.5$ GeV/c requirement on the lepton track. Clearly, the spectrometer must be designed to facilitate the trigger. For this study we have focused on the electron trigger but clearly both electron and muon triggers should be implemented (if practical).

4. The Spectrometer

The 1987 B spectrometer for the SSC shown in Figs. 2 and 3. The gross features are an intermediate (wide angle) spectrometer covering the rapidity range from 1.74 to 3.6, and a forward (downstream) spectrometer with rapidity coverage from 3.6 to 5.9. The intermediate spectrometer contains a 1.5 tesla-meter dipole, starting 1 meter downstream from the center of the interaction volume, and supplying a $p_\perp$ kick of 0.45 GeV/c to charged particles. All such charged particles will have traversed 6 silicon microstrip planes with perpendicular anode and cathode readouts, leading to 12 high-resolution position measurements before the particle enters the magnetic field. The microstrip detectors in combination with the two downstream drift chamber tracking stations will result in a momentum resolution of

$$\Delta p/p \sim 3 \times 10^{-3} + 10^{-4} p$$

for the intermediate spectrometer. The corresponding mass resolution $\Delta m/m$ will be $\sim$0.6% for typical 30 GeV particles.

Particles produced at angles smaller than 0.057 radians go into the forward spectrometer, passing through a 4.5 tesla-meter dipole and three drift chamber tracking stations. These particles receive a total $p_\perp$ kick of 1.8 GeV/c. The

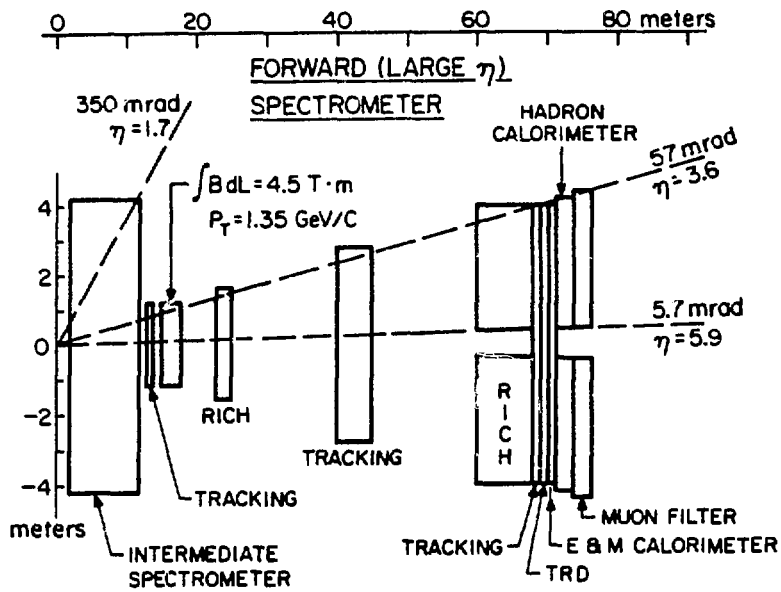

Figure 2. The 1987 B spectrometer. To set the scale, the electromagnetic calorimeter is located 70 meters from the beam crossing point and has transverse dimensions of ±4 meters. The upstream (intermediate) spectrometer is shown in Fig. 3.

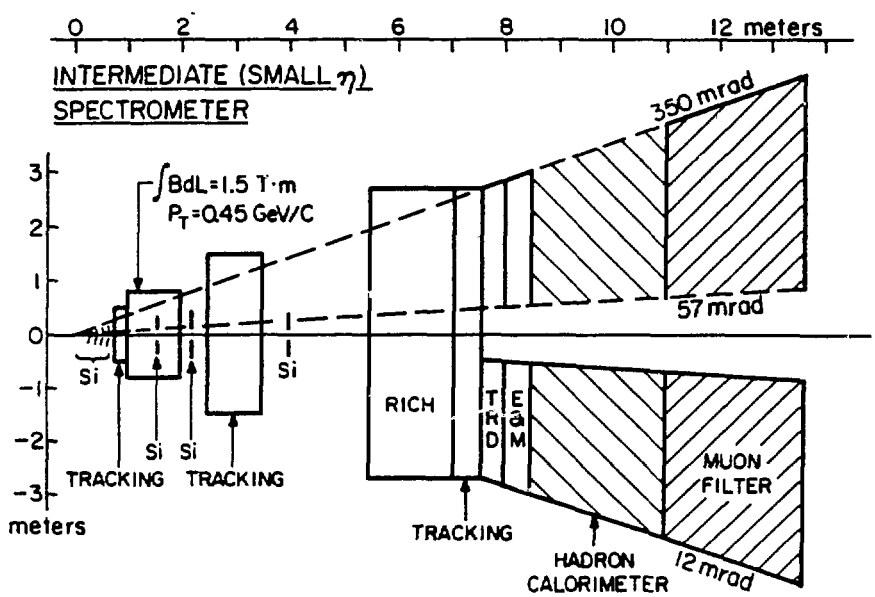

Figure 3. The intermediate beauty spectrometer. To set the scale, the electromagnetic calorimeter is 8 meters from the crossing point and has transverse dimensions of ±3 meters.

momentum resolution,

$$\Delta p/p \sim 1.5 \times 10^{-3} + 1.3 \times 10^{-5} p \ ,$$

corresponds to a mass resolution of ~0.3% for particles of typically 100 GeV.

Vertex finding, tracking, hadronic and leptonic particle identification, and other issues are discussed in the following sections.

i. Vertex finding and the beam pipe

Precise vertex resolution is absolutely essential for doing B physics at the SSC. In the absence of multiple Coulomb scattering the spatial resolution of a track at a vertex would be

$$\Delta x \simeq \sigma_o \sqrt{n} \Delta S / \Delta L \ ,$$

where σ_o is the intrinsic spatial resolution of a vertex tracking device plane, n is the number of planes per view, ΔS is the distance from the vertex to the first plane and ΔL is the distance from the first to the last plane. Unfortunately, the contribution from multiple Coulomb scattering may dominate. This contribution is

$$\Delta x^{ms} = 0.014 \frac{\Delta S}{p} \sqrt{X/X_0} \ ,$$

where p is the momentum in the GeV/c and X/X_0 is the thickness of the relevant material in radiation lengths. Since the transverse distance from the beam (R_T) is $\Delta S \tan\theta$ and $p_\perp = p \sin\theta$ ($\approx p \tan\theta$), the expression can be conveniently rewritten as

$$\Delta x^{ms}(\mu\text{m}) = \frac{7.6}{p_\perp(\text{GeV})} \ R_T(\text{cm})$$

for X/X_0 for a 300 μm silicon plane. To do B physics it is essential that Δx^{ms} be much less than $c\tau$ for beauty (~300 μm). Since the beauty decay particles have $p_\perp \sim$ 1–2 GeV/c, the first planes must be very close to the beams and multiple scattering in the beam pipe must be small.

Due to the practical difficulties in operating vertex detectors inside the beam pipe we considered placing the detectors outside the beam pipe with various beam pipe arrangements. The minimum beam pipe inner dimensions summarized in Table 1 indicate that the beam pipe inner diameter could be 1.0 cm to 1.2 cm for the first 60 m. (These requirements allow for an aperture-filling beam during filling, and guarantee that any beam scraping will occur elsewhere in the machine.) A 1 cm Be beam pipe could be 0.3 mm thick ($0.9 \times 10^{-4} X_0$) with a structural safety factor of three.

For such a straight cylindrical beam pipe the spatial resolution at the vertex just due to multiple scattering in the pipe is

$$\Delta x^{\text{beam pipe}}(\mu\text{m}) \sim \frac{4\,R_T(\text{cm})}{p_\perp(\text{GeV})}\frac{1}{\sqrt{\theta}}\,.$$

This is probably acceptable for the angles of the intermediate spectrometer such that $1/\sqrt{\theta} \lesssim 4$. For more forward angles a complicated beam pipe shape will be necessary. A number of beam pipe styles were proposed (see Fig. 4), but the optimal shape remains unclear.

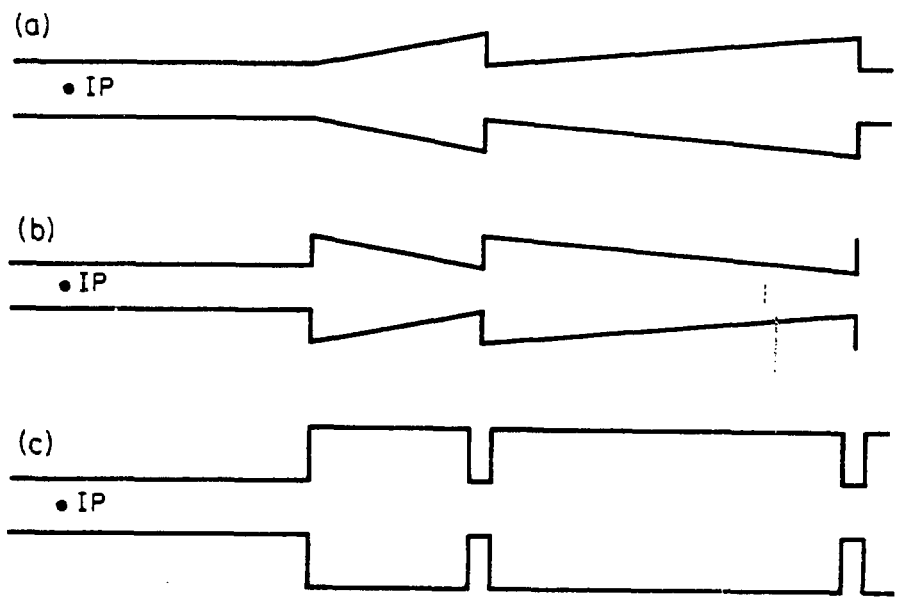

Figure 4. Three classes of ideas for beam pipe designs.

Independently of the beam pipe shape the organization of the vertex detector will be something like that shown in Fig. 5. The design is based upon currently available silicon microstrip type devices. Pixel devices are under active development [7] and could provide significant advantages. Figure 5a shows the approximate distribution of 15 of the 16 silicon microstrip stations along the beam line (the 16th is at about 4 meters from the interaction point). Each station is assumed to provide measurements in each of 4 views if silicon microstrips are used, or to provide a single high resolution pixel measurement if pixel devices are used. The distribution, designed so that each track registers in 3 stations, is approximately exponential.

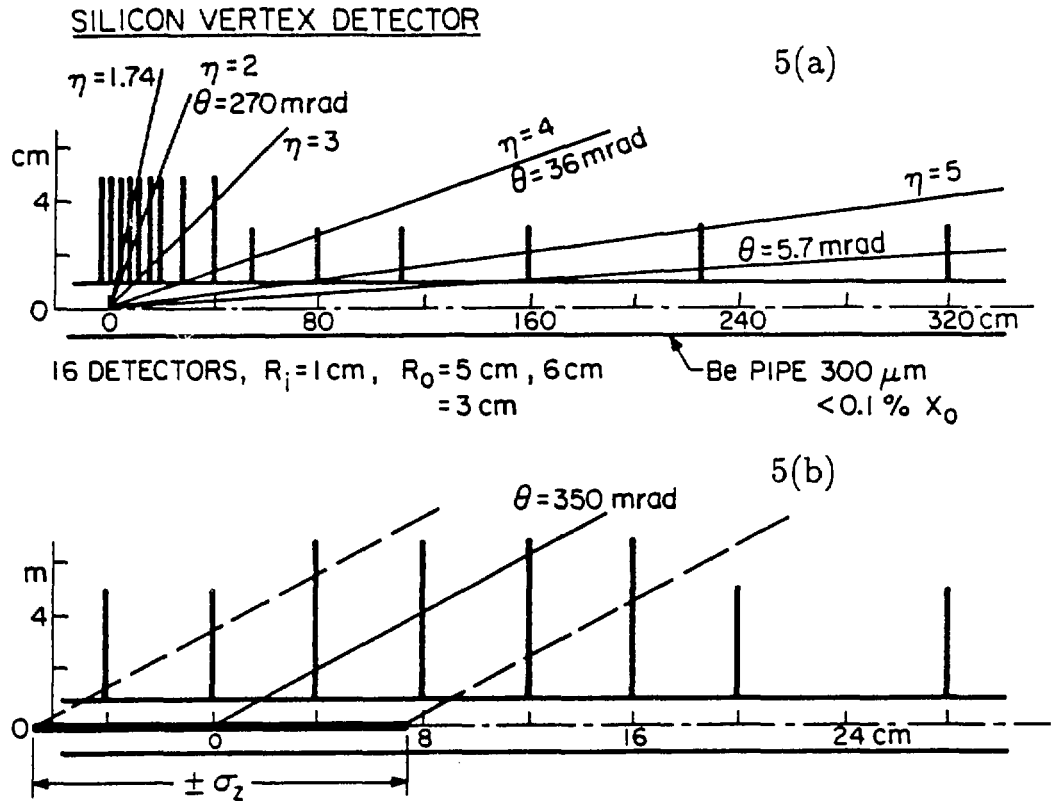

Figure 5. Schematic illustration of vertex detector arrangement. Fig. 5a shows 15 of the 16 measuring stations which surround the beam pipe. Each measuring station contains either 4 silicon microstrip views, or one pixel device. The detectors extend from an inner radius at the beam pipe of 1 cm to outer radii of 3, 5, and 6 cm as shown. Fig. 5b shows the area near the ±7 cm long beam interaction volume. The detector are actually tilted to be oriented as nearly perpendicular to the tracks as possible.

The problems associated with the long ($\sigma_z = \pm 7$ cm) collision region are evident from Fig. 5b, which shows the vertex detector arrangement near this region. While the detectors are tipped so that the average track is normal to the detector surface, there is still a sizeable spread in angles for these tracks, resulting in partial signals from a number of strips (or pixels).

For angles greater than about 20 milliradians the vertex tracking is accomplished with straight tracks in a nearly field free region. For particles at smaller angles, with momenta of typically 100 GeV/c, there will be some track curvature in the vertex detector.

Finally, we note that the vertex tracking system forms an essential part of the overall track finding and fitting. This is particularly true for the small angle

tracks, which intersect the first drift chamber trackers in regions of high occupancy.

If the vertex detector were made from double sided silicon microstrip detectors with 50 μm spacing as shown in Fig. 6, there would be approximately 2×10^5 strips. If pixel devices were used, with pixel sizes of 50 μm $\times$ 50 μm, there would be $\sim 2 \times 10^7$ pixels.

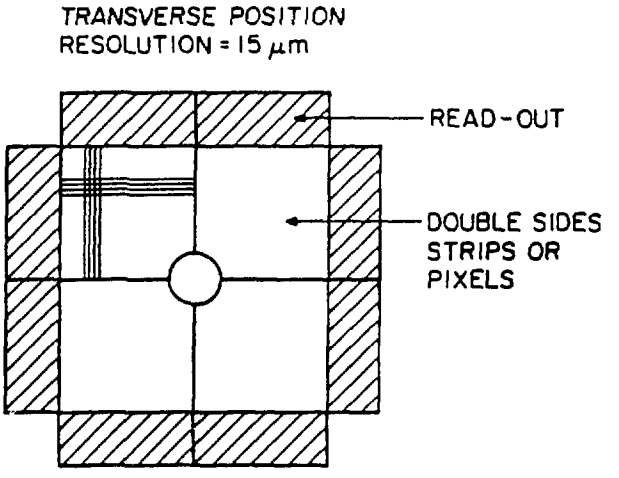

Figure 6. Beam's eye view of plane of silicon microstrip or pixel detectors.

ii. Magnets

The first magnet is a 1.5 tesla-meter dipole and has a ± 0.35 m entrance aperture in both the bend and non-bend directions. This aperture, which is located 1 meter from the center of the interaction volume, probably contains a mirror plate to terminate the fringe field. The downstream aperture must accept particles produced in a cone with 350 milliradian half angle. If the magnet is one meter long the exit aperture is ± 0.7 meters in size.

The second dipole magnet accepts tracks with angles < 57 mrad at a distance of 15 meter from the interaction point, and has a total field integral of 4.5 tesla-meters. The aperture of this magnet is ± 0.9 meters in both dimensions and the magnet is three to four meters long.

iii. Charged particle tracking

The tracking detectors must be highly redundant to achieve a high reconstruction efficiency and to be capable of handling the 10^7 s^{-1} event rate. The readout must be designed to provide fast triggering information. To facilitate track reconstruction in the trigger logic, the detectors have bend-plane and non-bend-plane views.

The design of the spectrometer is partially determined by occupancy considerations. With a charged particle multiplicity of 6 per unit of rapidity, a long chamber cell of width w a transverse distance R_T from the beam has a hit probability per event of

$$P = \pi w/R_T .$$

This gives a cell occupancy

$$O \simeq \frac{\pi w}{R_T}\left(1 + \frac{\Delta t}{\tau}\right) ,$$

where Δt is the relevant time resolution of the device and τ is the average time between events ($\sim$100 ns). For example, a 3 mm diameter cylindrical ("soda straw") cell with a drift speed of 50 μm ns^{-1} and with single hit electronics has a time resolution of 30 ns. Such a cell located 20 cm from the beam would have an occupancy of 6%. With larger cells and multiple hit electronics it is less clear how to define the relevant occupancy. If we define the effective width of such a cell as the double hit separation ($\sim$1 mm) and the time resolution as 1 mm/(50 μm ns^{-1}), then the occupancy of such a cell is again about 6%. It is clear that even with a luminosity of 10^{32}cm^{-2}s^{-1}, chambers cannot be effective at distances of less than about 15 cm from the beam. On the other hand, an infinitely long 50 μm wide silicon strip at $R_T = 1$ cm has an occupancy of $\sim$2% if the readout time resolution is 50 ns.

The tracking philosophy is evident from Figs. 2 and 3. Straight track segments are found by the silicon vertex detectors in the pre-magnet region where each track will have $\sim$12 high resolution points if silicon strips are used or 3 space points if pixel devices are used. In addition, the wider angle tracks will register in a pre-magnet chamber with very small cells. The main tracker for the wider angle tracks of the intermediate spectrometer is located about 3 meters downstream where these tracks are usually more than 20 cm from the beam. The main tracker might consist of a jet cell system, as shown in Fig. 7. There will be cells with x, y and 45° views, each composed of 16 sense wires with a half cell width of 6 mm. The sense wire planes are oriented at about 10° with respect to the forward track direction. Since a track always passes very close to at least one sense wire, there is a prompt signal which gives the track coordinate and the drift times from neighboring sense wires give the track angle. It might be necessary to reduce the cell spacing at small R_T due to the rates. This chamber contains about 11,000 sense wires. The final tracking device of the intermediate spectrometer is located just upstream of the TRD. This chamber helps in the tracking and improves momentum resolution. It is also required in the electron

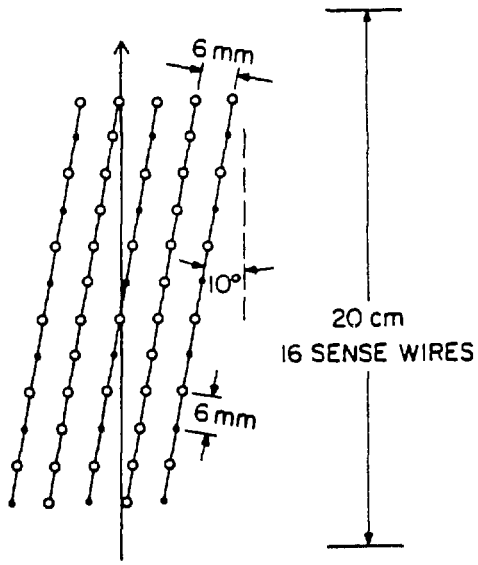

Figure 7. Cell structure of main drift chamber tracker.

trigger to reject photon conversion occurring in the TRD radiator. This tracker has ~6000 sense wires.

At less than 57 mrad particles go through the hole into the downstream spectrometer. A chamber at 13 meters, just before the big magnet, helps in linking tracks found in the downstream tracker with the pre-magnet segments found in the silicon. This chamber also helps with soft tracks which have inadvertently gone through the hole, and it helps identify "shine" off the edge of the hole. This chamber contains about 6000 small cells. At this location, the resolution obtainable with a high pressure straw chamber [10] would significantly improve the momentum resolution of high momentum tracks. The main downstream tracker is at about 40 meters. It is similar to that of the main intermediate tracker and contains about 20,000 sense wires. The occupancy of this device should be satisfactory at 20 cm from the beam, which corresponds to the 5.7 mrad acceptance limit. There is also a far-downstream chamber, just in front of the TRD, which helps with track finding, momentum resolution for high momentum tracks, and is important for the trigger. This device contains about 8000 wires. The estimated total number of sense wires in the charged particle tracking is about 55,000. Portions of wires closer to the beam than 10 cm are deadened.

It should be pointed out that this proposal for tracking is clearly one example of many possibilities. The main problems occur close to the beam where

occupancies are 5–10%. Linking the small angle tracks found in the downstream spectrometer to those found in the silicon might present problems. In this case somewhat more silicon could be installed at about 4–8 meters from the interaction point.

iv. Hadron particle identification

For B physics the identification of hadrons, and especially kaons, will be very important, probably essential. The two stage spectrometer greatly facilitates particle identification. Figs. 2 and 3 show three stages of ring-imaging Čerenkov (RICH) detectors, each of which has 32 photon detector planes. Table 2 indicates the basic physics properties of each detector. In the forward spectrometer $K\pi$ separation is achieved from 5–200 GeV/c and K/p separation is obtained from 6 to 370 GeV/c. For the intermediate spectrometer the corresponding momenta are 3–40 GeV/c and 10–70 GeV/c, respectively. The particle identification for the intermediate spectrometer can be extended to very low momentum via time of flight counters located near the electromagnetic calorimeter, 8 meters from the interaction point. At this distance 3 GeV/c K's and π's have a flight time difference of 0.36 ns, nearly identical to the time difference of 5 GeV K's and protons. These values are about 4 times larger than reported time of flight resolution (under 0.1 ns)[8].

Table 2

Properties of the three ring imaging Čerenkov counters. The table gives the difference of the index of refraction n from unity, the length of each counter in meters, the relevant momentum region for each in GeV/c, and the expected number of photoelectrons.

	1	2	3
$n-1$	1.7×10^{-3}	6×10^{-4}	6×10^{-5}
Length (m)	0.8	2.0	20
e/π	<12	<20	<60
π/K	3 - 40	5 - 70	15 - 200
K/p	10 - 70	6 - 120	50 - 370
# p.e.	25	25	25

A typical RICH cell contains an average of $\frac{1}{2}$ of a ring per interaction, i.e., an overall rate of ~10 MHz. The detector planes can be placed (via mirrors) at rather large distances from the beam to reduce radiation problems and the passage of minimum ionizing tracks. The electron rate at a sense wire is still very high, however. The planes can be read out in the same manner as in Fermilab

experiment E605[9], with a multistep proportional chamber. Finely segmented cathode pads may be necessary. Due to the concerns about TMAE related chamber degradation it may be necessary to develop a new readout scheme (perhaps segmented phototubes) or to use conventional threshold Čerenkov counters.

v. Transition radiation detectors

It is clear that a single lepton trigger will be essential for high rate B physics, and here we consider the case of an electron. In addition to greatly helping with electron identification offline, transition radiation detectors (TRDs) are crucial in making fast electron trigger decisions.

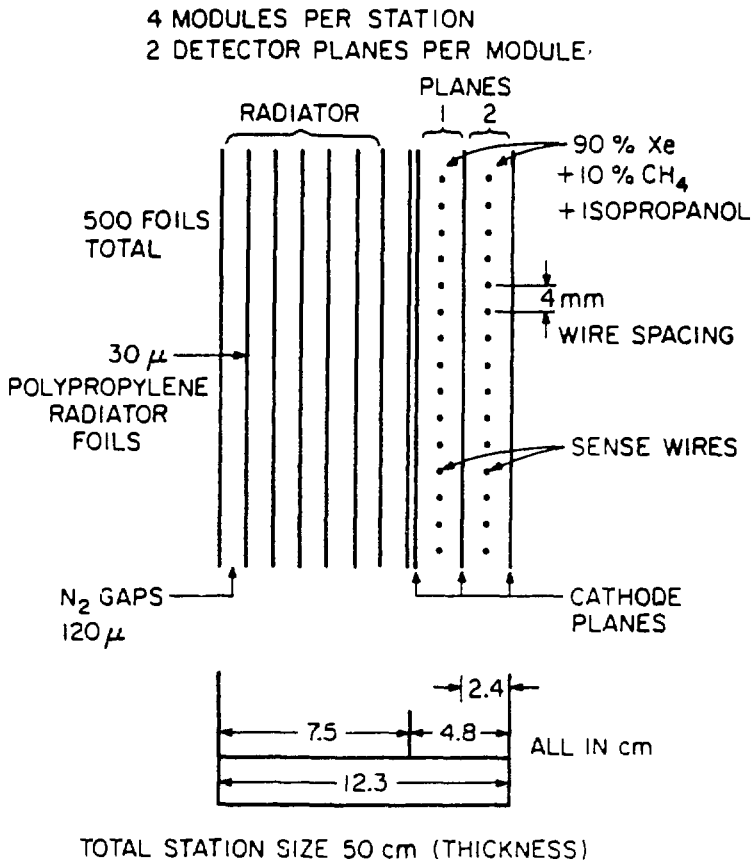

Figure 8. Schematic design of one transition radiation detector. There are four modules per TRD detector.

The TRDs are located just upstream of the electromagnetic calorimeter. Each is composed of 4 modules. As shown in Fig. 8, each module contains 500 thirty-

micron polypropylene foils separated by 120 μm nitrogen gas gaps. The average of two TRD photons produced per module are detected in the two 90% Xe +10% CH_4 gas detectors. Two detectors are chosen, each with an absorption probability of 0.5 for each module, to reduce the total drift collection time to 600 ns. The electronics are just sensitive to large ionization clusters and OR the two detectors. Demanding that 3 of the 4 modules has a cluster, results in a 90% efficiency for counting electrons with a rejection of better than 1/50 for pions of momenta less than 100 GeV. Figs. 9a and 9b illustrate a scheme for arranging a mosaic of smaller detectors to cover the large required areas. The wires are ganged to minimize the number of readout channels while maintaining a reasonable occupancy. The distribution of channels is given in Table 3. An estimated 23,000 anode channels are needed.

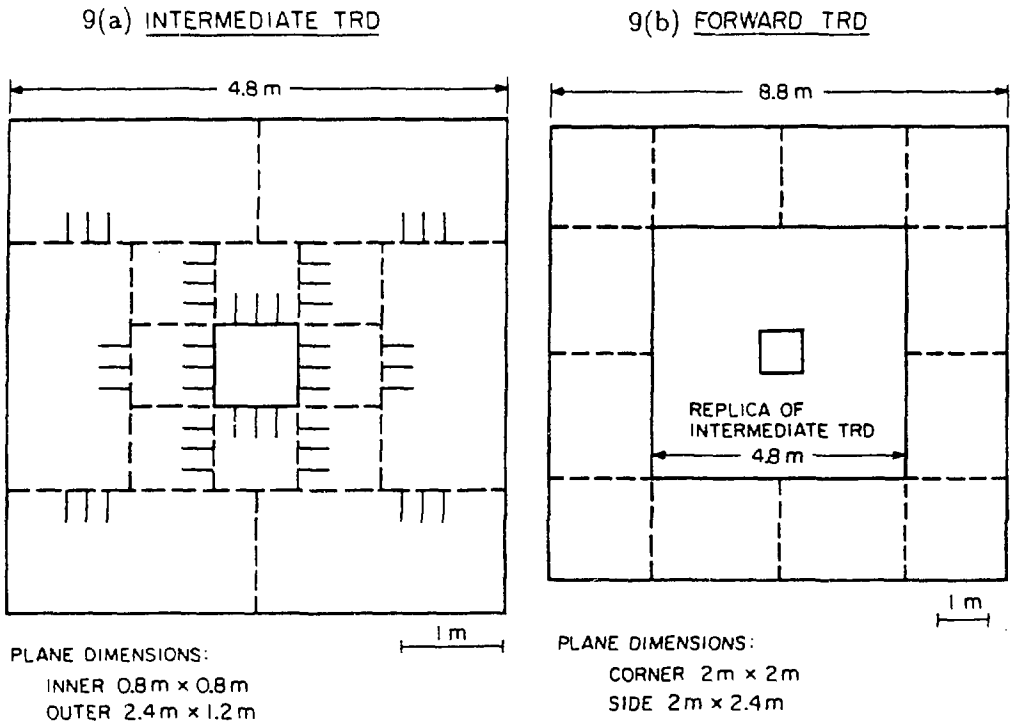

Figure 9. Schematic of the mosaic arrangement of TRD detectors to cover the large required areas of the intermediate (Fig. 9a) and forward (Fig. 9b) detector.

It may also be advantageous to read out cathode pads which are geometrically matched to the towers of the electromagnetic calorimeter. Finally, we note that since the readout is supposed to be sensitive only to the signal clusters associated

with the large local ionization from the absorbed x-rays, the occupancy of the TRD should in general be rather low. This will reduce problems caused by the long drift time in xenon.

Table 3
Distribution of TRD channels.

TRD	Chamber type	Chambers per plane	Wires per plane	Ganging factor	Channels per plane
Intermediate					
	Inner	8	1600	4	400
	Outer	6	3600	6	600
					1000
Summary:	1000 channels/sense plane				
	8000 total channels				
Forward					
	Outside corners	4	2000	8	250
	Outside sides	8	4800	8	600
	Replica of inner TRD				1000
Summary:	1850 channels/sense plane				
	14,800 total channels				
	Total of 22,800 channels for the entire spectrometer				

vi. The electromagnetic calorimeter

The main functions of the electromagnetic calorimeter for high rate B physics are electron identification and helping facilitate the electron trigger. As a consequence, transverse and longitudinal segmentation are very important. Energy resolution is important in that it helps with the electron identification, but superb energy resolution is not a necessity. It would be nice to reconstruct B-decay π^0's. However, since the efficiency for finding π^0's in these many-particle events will be small and the backgrounds large, and since π^0's do not leave tracks in vertex detectors, it is highly unlikely that π^0 reconstruction will be very useful.

Two considerations determine the transverse segmentation of the detector. The first is occupancy. The probability per event that a detector element of area dA at a transverse distance R_T from the beam is hit is $dA/R_T^2 = \Delta\eta\Delta\phi$. The occupancy for charged particles or photons then is $(dA/R_T^2)(1+\Delta t/\tau)$, where Δt is the time resolution of the detector and τ is the average time between collisions ($\sim$100 ns). To fix ideas, we consider a lead-liquid argon device with narrow gaps

and assume that $\Delta t \sim 200$ ns has been achieved through the addition of methane. If we wish to restrict the occupancy to $\alpha = 0.002$, then the size of a transverse cell should be $dA = \alpha R_T^2/(1+\Delta t/\tau)$. The number of cells in an annulus of radius R_T and width ΔR_T is $\Delta N = (2\pi/\alpha)(1+\Delta t/\tau)\ \Delta R_T/R_T$. For a detector with inner radius R_T^{min} and outer radius R_T^{max} we then need a total number of cells

$$N = (2\pi/\alpha)(1+\Delta t/\tau)\ \ln(R_T^{max}/R_T^{min})\ .$$

For the downstream detector, $R_T^{min} \sim 30$ cm and $R_T^{max} \sim 4$ meters, so $N \simeq 24,000$ cells. Faster time resolution (e.g. $\sim$50 ns) could reduce the number of cells by a factor of two. A less stringent occupancy criterion could also reduce the total.

A second criteria is that of shower size. For a lead-liquid argon calorimeter the 90% containment radius is $\sim$2 cm. There is not much reason to make a cell smaller than about 1.4 cm $\times$ 1.4 cm, since this is the intrinsic shower size. On the other hand, much of the pion rejection is obtained by observing a narrow shower and by comparing the shower location with that of the incident charged particle. The shower position can be obtained to $\sim$1 mm precision in a fine-grained calorimeter, and this leads to a powerful rejection of pion-photon overlaps. To obtain both the width information and the shower position, shower segmentation should be comparable to the shower width.

The two criteria agree at a radius such that

$$\begin{aligned} R_T &= \sqrt{(1.4\text{ cm})^2\ (1+\Delta t/\tau)/\alpha} \\ &= 53\text{ cm}\ . \end{aligned}$$

For smaller radii the occupancy is larger than our 0.002. At $R_T = 30$ cm it is 0.006, which is still acceptable. For larger radii the shower width criterion is the more stringent.

To satisfy both criteria while keeping the number of segments (and therefore the cost) down, a hybridized scheme is suggested for use at larger R_T. Towers will be designed according to an occupancy rule, interleaved in alternating layers with x and y strips whose width is determined by the transverse shower size. In addition, each tower is segmented into 3 longitudinal segments to further aid in pion rejection.

A quadrant of the forward electromagnetic calorimeter is shown in Fig. 10. Within the region where x and y are less than 1 meter from the beam there are a total of 20,408 towers, each 1.4 cm square, and each segmented longitudinally

into three readouts. For x and y between 1 m and 2 m there are 7890 towers, each 3.9 cm square and segmented longitudinally for three readouts. In this region tower layers are interleaved with x and y strip layers 1.3 cm $\times$ 11.7 cm. The outer region contains larger towers and strips, as indicated in Table 4. The total thickness of the detector is about 35 radiation lengths and each layer is about 0.5 radiation lengths thick. The total weight of the detector is about 140 tons.

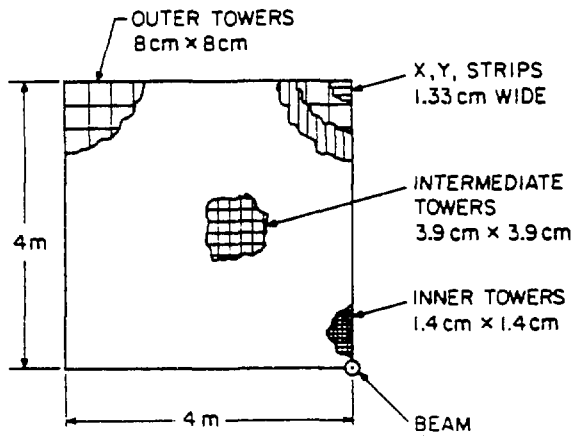

Figure 10. A schematic view of one quadrant of the forward electromagnetic calorimeter. For larger distances from the beam a hybrid cell structure is chosen with projective towers, x strips and y strips in alternate layers.

The electromagnetic calorimeter for the intermediate detectors is very similar but smaller. The weight is about 80 tons and there are 116,300 readouts.

vii. Hadron calorimeter and muon detector

The primary purpose of the hadron calorimeter is to help with electron and muon identification. As a consequence a simple iron calorimeter is adequate. This calorimeter is followed by an iron muon filter.

The first two interaction lengths mainly serve to help with the electron identification and are arranged in towers, with two samples per interaction length. Each tower matches four of the electromagnetic towers and is used in the electron trigger to veto hadrons which otherwise appear to be electrons. There are about 9000 and 8000 towers, respectively, for the forward and intermediate calorimeters. This section of the calorimeter might also contain liquid argon and would then share a cryostat with the electromagnetic calorimeter.

Table 4

Distribution of electromagnetic calorimeter readouts for the forward spectrometer. The intermediate spectrometer has somewhat fewer channels.

Type	Size	Minimum x or y	Maximum x or y	Longitudinal Segments	Number of Readouts
Towers	1.4 cm × 1.4 cm	0	1 m	3	61,224
Towers	3.9 cm × 3.9 cm	1 m	2 m	3	23,668
x strips	1.3 cm × 11.7 cm	1 m	2 m	1	7,890
y strips	1.3 cm × 11.7 cm	1 m	2 m	1	7,890
Towers	8 cm × 8 cm	2 m	4 m	3	22,500
	1.3 cm × 48 cm	2 m	4 m	1	7,500
	1.3 cm × 48 cm	2 m	4 m	1	7,500
					138,172

The remainder of the hadron calorimeter, composed of 10 interaction lengths of iron, is designed to help with muon identification and with muon tracking for a single or dimuon trigger. It is read out in 20 sampling layers, using a combination of plastic scintillators for fast timing and gas chambers with anode wire and cathode pad readout for position measurement. The readout configuration has yet to be completely defined. The iron weighs 900 tons for the forward hadron calorimeter and 600 tons for the intermediate calorimeter.

The iron muon filters are each 1.8 meters thick, with a total of four layers of drift chamber readout for muon tracking within and behind the iron. The weight of this iron is about 900 tons for the forward and 700 tons for the intermediate stage. There is clearly space for a longer filter for the forward spectrometer, should it be required.

viii. Acceptance for K_s's

Here we make a very rough estimate acceptance for K_s decay particles. We assume that a K_s must decay before or within a magnetic field to be identified. The typical decay distance L is $\gamma\beta c\tau$. With a $p_\perp$ of a K_s from B decay of about 1.5 GeV/c and with $\gamma\beta \sim p_\perp/\theta M$ we have $L\theta \sim 9$ cm for a K_s decay. A K_s produced at an angle greater than 0.057 radius must decay before about 1.5 meters in order for the decay mesons to be magnetically analyzed. The worst case for these particles is at the edge where the K_s's are fastest. The mean decay distance at 0.057 radians is ~9 cm/0.057 = 1.5 m. At this worst angle about half of the K_s's are accepted.

Similarly, at the inner acceptance of the forward spectrometer the mean decay distance is 15 meters, which is again comparable to the distance to the second magnet. We conclude that the acceptance for K_s's exceeds 75%.

ix. Shine from the hole

In a typical event, the probability that a particle hits the intermediate calorimeters within a distance ΔR_T of the inner hole is about $2\pi\Delta R_T/R_T$ for both photons and charged particles. For photons, we expect some downstream shine when ΔR_T is less than the transverse electromagnetic shower width. The same is true for hadrons when ΔR_T is less than the corresponding width for hadronic showers.

To minimize both effects the inner edge regions of the intermediate calorimeters should be made as compact as possible with tungsten absorber and perhaps silicon readout materials. In tungsten the 90% containment radius is about 1 cm for electromagnetic shower and about 4 cm for hadronic cascades. We then expect that about 13% and 50% of the events will have a photon and a charged hadron, respectively, within the 90% containment radius. (The hadronic fraction should be increased somewhat to account for neutral hadrons).

For events at the 90% containment radius, about 3% of the energy escapes into the hole and produces shine. Typical energies for the edge particles are about 70 GeV, so we might expect about 2 GeV in this shine. This shine will be more or less isotropic and will generate noise in nearby chambers. When the particle strikes nearer to the edge the shine will be more directional and energetic. The biggest problem will occur in the chambers just upstream of the second magnet. These chambers subtend a solid angle which is about $4\pi/50$.

The problem of shine from these interactions deserves a much more careful study. It appears from this very quick look that shine will be a nuisance, but not a major problem.

5. Rates

The crucial question is whether the experiment would produce enough clean, tagged B decays to observe CP violation in a few separate channels. We have chosen those channels which have large asymmetries and have clean experimental signatures. Unfortunately, they also have small branching ratios, but it is unrealistic to think that it will be easier to see smaller CP-violating-effects in more common modes. The efficiencies can only be estimated at present, but such estimates are useful to reach a preliminary number for the sensitivity.

The goal is to collect events of the type $B^0 \to \psi K_s$ (or $\pi^+\pi^-$) with $\overline{B} \to De\nu$ ($D^*e\nu$). The geometric acceptance for all particles, including the requirement

$p_\perp \geq 0.3$ GeV/c, is about 0.05. The branching ratio for one of the semileptonic decays is about 20%, and the fractions of D's decaying into modes with two more charged particles and no neutrals is about 20%. The branching ratio product for $B^0 \to \psi K_s$, $\psi \to e^+e^-$ and $K_s \to \pi^+\pi^-$ is about 5×10^{-5}, and the branching ratio for $B^0 \to \pi^+\pi^-$ may not be much different. The product of all these factors is about 10^{-7}. Efficiencies for vertex cuts, reconstruction, and particle identification are similar to existing experiments, and might be about 0.2, which gives a total factor for acceptance, efficiency, and branching ratios of 2×10^{-8}.

A cross section of 200 μb for $B\overline{B}$ and a luminosity of $10^{32}\,\mathrm{cm}^{-2}\mathrm{s}^{-1}$ $\mathrm{cm}^{-2}\mathrm{s}^{-1}$ means a total of about 2×10^{11} $B\overline{B}$ pairs in a running year of 10^7 seconds. This would give about 4000 B events in each of the rare modes in which a large asymmetry is expected, with a well-identified $\overline{B}$. The studies of the B-physics subgroup show that about 2000 events of this type are sufficient to see significant CP violation, assuming an asymmetry of about 0.1. The other factor that needs to be taken into account is that part of the trigger efficiency not included in the requirement of a high $p_\perp$ electron within the spectrometer acceptance. There must be more detailed work on the triggers before such effects can be estimated. For the particular case of the ψK_s mode, a dilepton trigger can probably be used without further loss. However, it is important to look at modes which require single-lepton triggers.

Observing 4000 B events per channel for 2×10^{11} $B\overline{B}$ pairs is somewhat more pessimistic than the conclusions of many studies of the CP problem in B decays. This is partly because special modes are used which have ideal properties for CP violation, but small branching ratios. Since the fraction of events with $B\overline{B}$ production is 2×10^{-3}, the series of cuts used may be more restrictive than needed. It is quite possible that it is not necessary to see a decay mode of the D with no neutrals to be able to clearly identify the semileptonic B decay. It may also be possible to sum over particular modes which have the same sign for their asymmetries.

At present we choose to take the most conservative approach, which demands a high rate. It is worth noting that even at an e^+e^- machine with vertex detection, where a trigger is not needed, a similarly conservative calculation shows that about 10^9 produced $B\overline{B}$ pairs are needed.

6. Cost Estimates

The cost estimates for most of the components of the beauty spectrometer have been made using the standardized costs from the Report of the Detector Cost Evaluation Panel[11], and are given in Table 5 below.

Table 5

Estimated cost of the beauty spectrometer.

Item	Cost in K$	
1. Electromagnetic Calorimeter		
A. Forward		
140 tons at $9	1,260	
Electronics 138 K channels at $120	16,560	
		17,820
B. Intermediate		
80 tons at $9	720	
Electronics 116 K channels at $120	13,920	
		14,640
2. Tracking		
55 K wires at $100	5,500	
Electronics 55 K channels at $120	6,600	
		12,100
3. Hadron Calorimeter and Muon Filter		
A. Forward		
L.A. section 300 tons at $9	2,700	
Other section 600 tons at $3.5	2,100	
Electronics 18 K channels at $120	2,160	
Muon Filter iron 900 tons at $3.5	3,150	
4 K wires at $100	400	
4 K channels at $120	480	
		10,990
B. Intermediate		
L.A. section 200 tons at $9	1,800	
Other section 400 tons at $3.5	1,400	
Electronics 16 K channels at $120	1,920	
Muon Filter iron 700 tons at $3.5	2,450	
4 K wires at $100	400	
4 K channels at $120	480	
		8,450
4. Cryogenics for liquid Argon		2,000
5. RICH		
Mechanical	6,000	
Electronics	7,000	
		13,000

6. TRDs			
	23 K channels at \$120	2,760	
	23 K ganged wires at \$100	2,300	
			5,060
7. Vertex Detector			
	2×10^5 strips at \$20 each		4,000
8. Magnets			2,000
9. On-Line Computing			2,500
10. EDIA			25,000
	Total Cost		117,560

7. Conclusion

The purpose of this study was to examine the feasibility of studying B physics at very high rates, with a definitive CP violation experiment as the ultimate goal. We found no problems of a fundamental nature in achieving this goal.

On the other hand, this experiment demands detectors which work at rates well beyond those commonly used in high energy physics. These are a number of questions about radiation hardness that need more work. There are also more subtle problems, such as effects of high rates on tracking efficiency, electron identification, etc. There are also possible solutions involving finer segmentation, faster elements (as suggested in the electron trigger study) and in some cases more clever design. There must be more detailed study of these problems to see in which cases the additional expense of a more elaborate detector is justified.

Major design choices included the acceptance angles for the two spectrometers. This problem deserves further attention in future workshops. The detectors need to be larger in the bend-plane dimension to accept the charged particles with low momentum. Already the transverse sizes of the calorimeters are quite large. The size of the forward spectrometer can be reduced by either making the hole in the intermediate spectrometer smaller or by moving the forward spectrometer closer to the interaction point. In the first case, the bad effects at the edge of the hole become more serious and the intermediate detector must operate closer to the beam pipe. Moving the forward detector closer to the interaction region reduces the acceptance of the spectrometer at small angles. A possible alternative that might be less expensive and easier is a three-stage spectrometer, but then there is a second edge to contend with. Finally, it would help if larger angles could be accepted by the intermediate spectrometer. All of these are important issues that need detailed study and should be addressed in the future. For this study, we assumed vertex detectors outside the beam pipe because they

are easier to build and maintain. This does have some negative consequences on the vertex resolution, on pair backgrounds for the electron trigger, and for the generation of secondary hadrons. It appears that these effects are tolerable except perhaps at the smallest angles accepted. Although some effort was spent on producing better beam pipe-vertex detector designs, it became apparent that this would also take more study.

In order to do the definitive CP experiment, it is necessary to measure CP violation in many modes. This requires single lepton triggers which do not make any restriction on the decay mode being studied. (Only particles from the opposite-side $\overline{B}$ are used in the trigger.) This requires some information from the vertex detectors as well as clean lepton identifications. It is also necessary to select 100 to 1000 events s^{-1} from total event rate of 10^7 s^{-1}. Such a requirement makes demands on the readout electronics, triggers, input/output devices, and data analysis system which are truly unprecedented. The most important outstanding question is the extent to which an ambitious but realistic trigger and data acquisition system will limit the physics results.

To summarize our results, it is reasonably safe to conclude that the SSC will be a good place for a high-rate B experiment. The fraction of events which contain a $B\overline{B}$ pair is larger than the fraction of events in fixed target hadron production which contain charm. Recent experience with fixed target charm production experiments indicates that there is no serious question about the availability of clean bottom meson samples at the SSC. With 2.5×10^{11} $B\overline{B}$ events produced each year, the size of clean B signals should be beyond that available at any other presently proposed machine, even after accounting for trigger losses.

The second major conclusion is that a forward spectrometer is needed to obtain the desired acceptance. One should take the broadest view of forward, however. It is important to accept the largest rapidity slice possible, keeping in mind that this means within the prime performance region of the detector.

The spectrometer elements are relatively conventional, and nothing outside our present technology is required. There are a series of critical experimental issues, enumerated above, that need further study. The single leptonic triggers are possibly the most challenging problems.

In summary, the prospects that the definitive experiment on CP violation in the $B\overline{B}$ system will be built at the SSC are quite good. Given the central nature of this problem for our understanding of the standard model, it is worth pursuing the design of such an experiment. A fresh look at the problems in the next workshop should produce a design which more closely approaches a realistic experiment.

References

1. K. J. Foley *et al.*, "Bottom and Top Physics," these proceedings.
2. R. J. Morrison, S. McHugh, and M. V. Purohit, "A Semileptonic Electron Trigger for Recording $B^0\overline{B^0}$ Events," these proceedings.
3. L. J. Gutay, D. Koltick, J. Hauptmann, D. Stork, and G. Theodosiou, "Intermediate $p_\perp$ Jet Spectrometers, these proceedings.
4. L. W. Jones, "A Small-Angle Spectrometer Addition to the Intermediate-$p_\perp$ B Spectrometer," these proceedings.
5. B. Cox and D. E. Wagoner, pp. 83–91, *Physics of the Superconducting Supercollider*, ed. by R. Donaldson and J. Marx (Snowmass CO, 1986).
6. B. Cox, F. Gilman, T. D. Gottschalk, pp. 33-44, *Physics of the Superconducting Supercollider*, ed. by R. Donaldson and J. Marx (Snowmass CO, 1986).
7. Talks by David Nygren, Sherwood Parker and Steve Shapiro at this Workshop.
8. W. Reay, private communication (1987).
9. M. Adams *et al.*, Nucl. Instr. Meth. **217**, 237 (1983), and H. Glass *et al.*, IEEE Trans. Nucl. Sci. **NS-32**, 692 (1985).
10. R. DeSalvo, "A proposal for an SSC Central tracking detector", Cornell University Laboratory of Nuclear Studies report CLNS 87/52 (1987).
11. "Cost Estimate of Initial SSC Equipment", SSC Central Design Group Report SSC-SR-1023 (1986).